



# Inferring multi-scale neural mechanisms with brain network modelling

**Michael Schirner<sup>1,2,3</sup>, Anthony Randal McIntosh<sup>4</sup>, Viktor Jirsa<sup>5</sup>, Gustavo Deco<sup>6,7,8,9</sup>,  
Petra Ritter<sup>1,2,3,10\*</sup>**

Yile Wang

Brain Dynamics Journal Club Presentation

# Outline

- This paper provides a new simulation method of combining experimental data with theories about how the nervous system works.
- Alpha-band oscillation (8-12hz) is involved in multiple information processing. The observed inverse relationship between alpha-band and neural firing is central to hypotheses to “gating by inhibition” and “pulsed inhibition”.
- Power-law distribution in critical dynamics in brain

Fig 1. Modeling framework

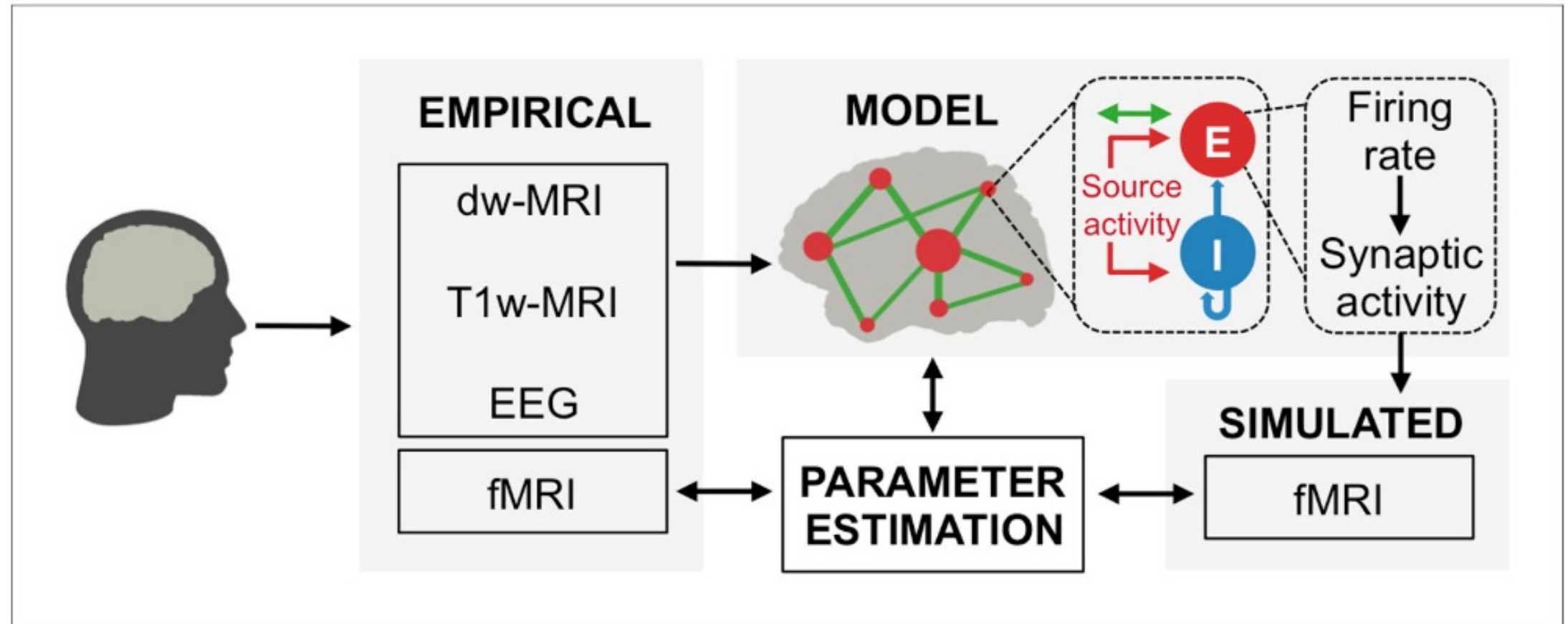


# Fig 2. Reproduce a variety of empirical works

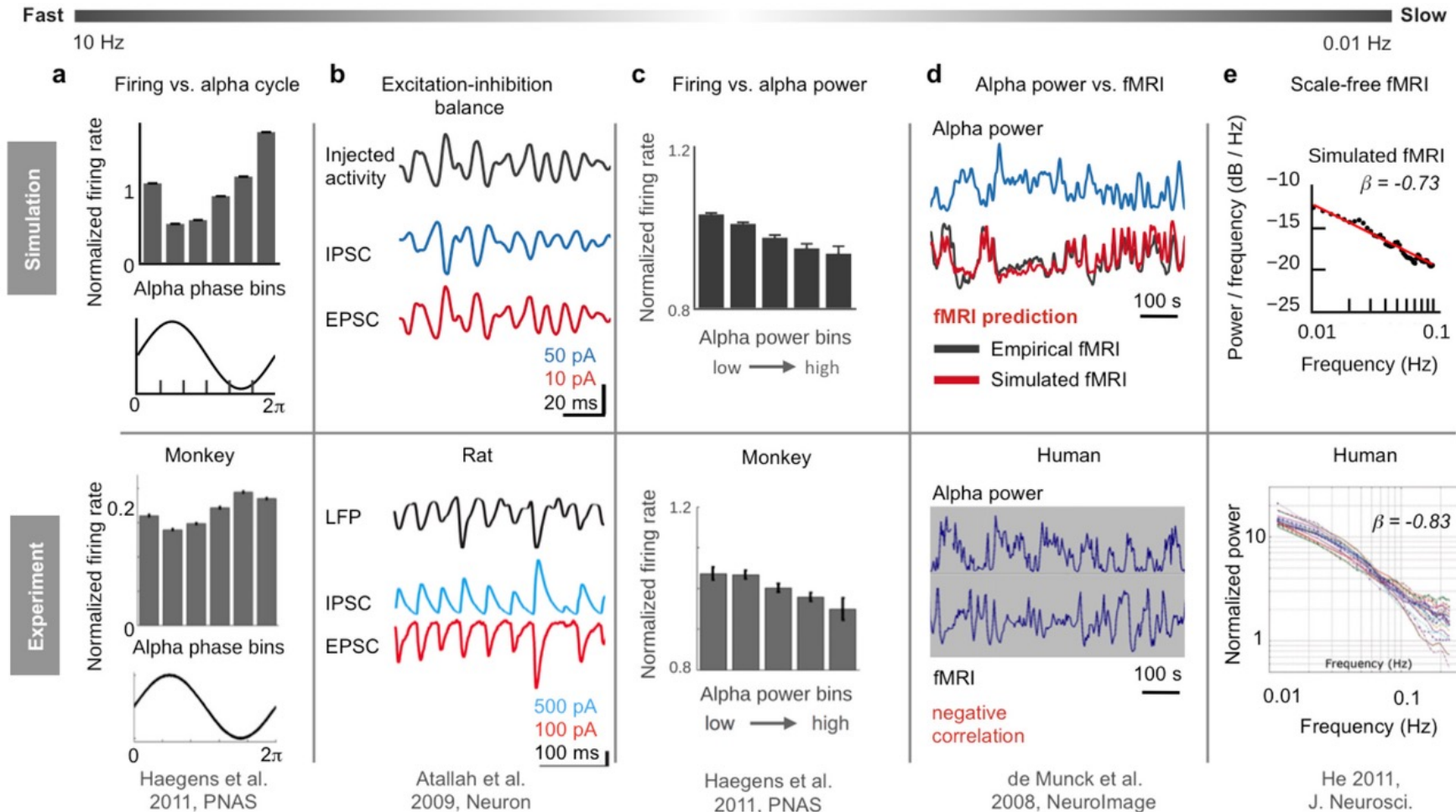


# Fig 3. Individualized predictions of ongoing resting-state fMRI

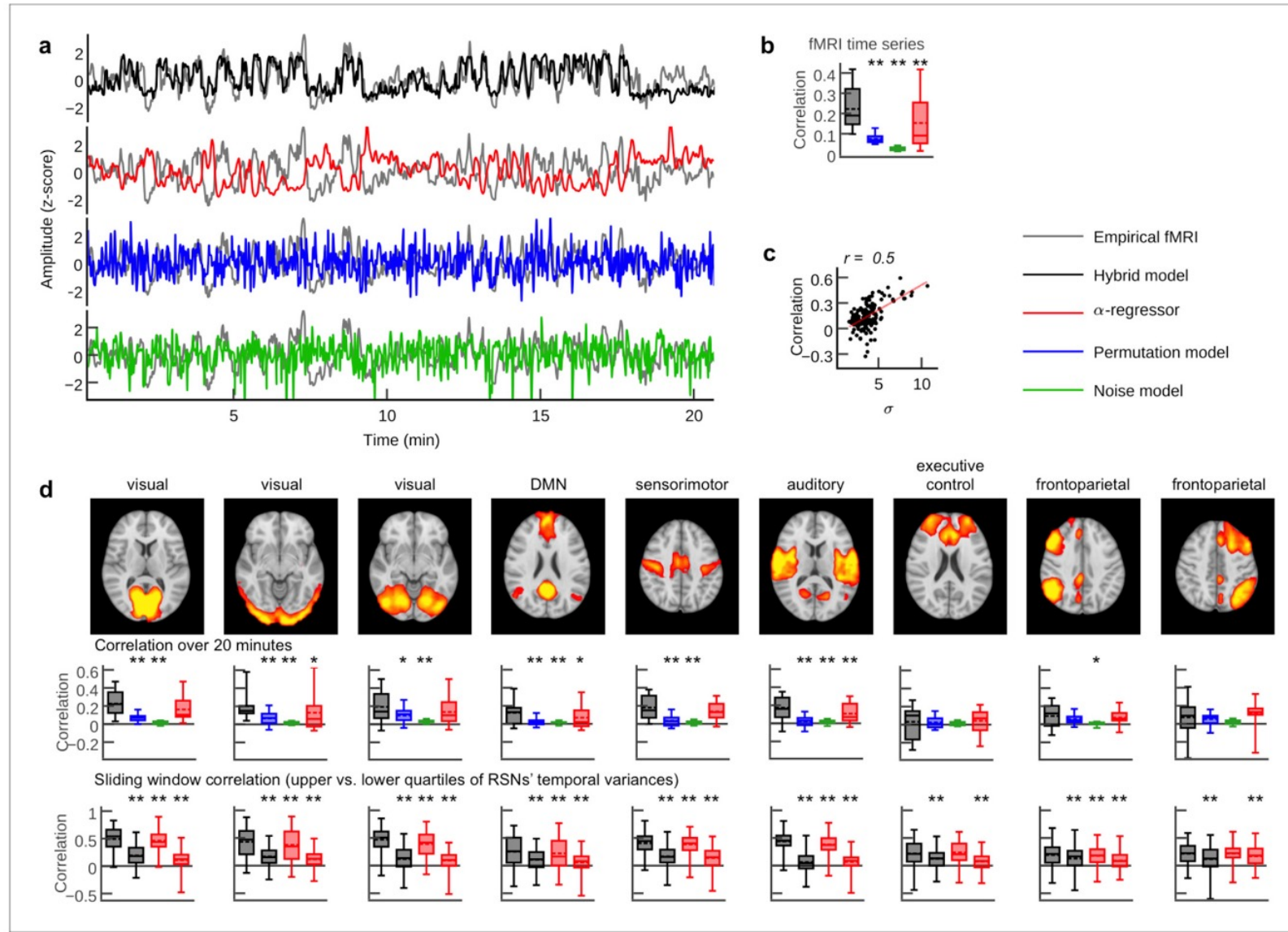


# Fig 4. Functional Connectivity Prediction

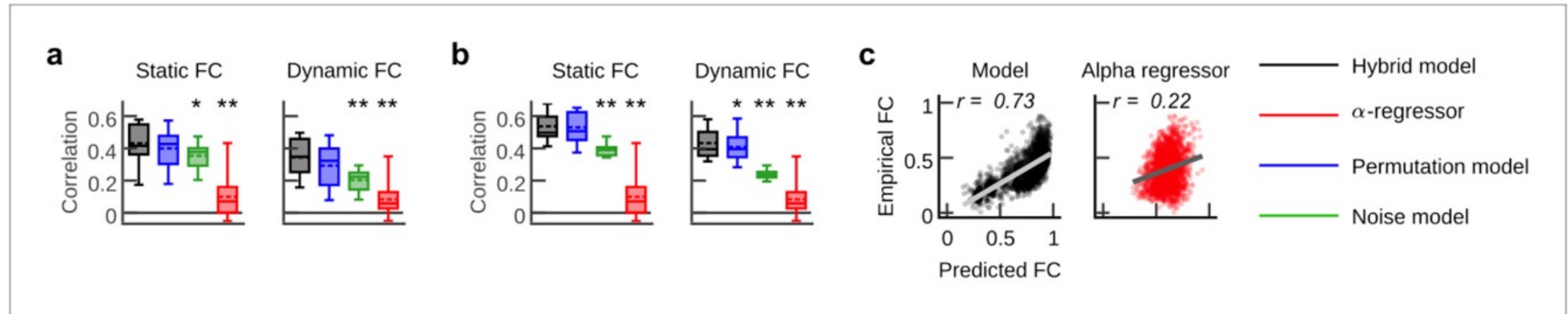


**Figure 4.** Functional connectivity prediction. (a, b) Box plots show correlation coefficients obtained from correlating all subdiagonal entries of empirical and simulated FC matrices. FC was computed for long epochs (static FC; computed over 20.7 min) and short epochs (dynamic FC; average sliding window correlation; 100 fMRI scans window length; one fMRI scan step width). Results were compared for (a) the parameter set that generated the best fMRI time series prediction and (b) the parameter set that yielded the best FC predictions for each subject. (c) Scatter plots compare empirical and simulated average FC for hybrid model simulations and the  $\alpha$ -regressor. Dots depict all pair-wise region time series correlations averaged over all subjects. Asterisks in (a) and (b) indicate significantly increased prediction quality of the hybrid model compared to control conditions in one-tailed Wilcoxon rank sum test (\* $p < 0.05$ , \*\* $p < 0.01$ ).

DOI: <https://doi.org/10.7554/eLife.28927.007>



Fig 5. E/I balance generates the inverse relationship between  $\alpha$ -phase and firing.

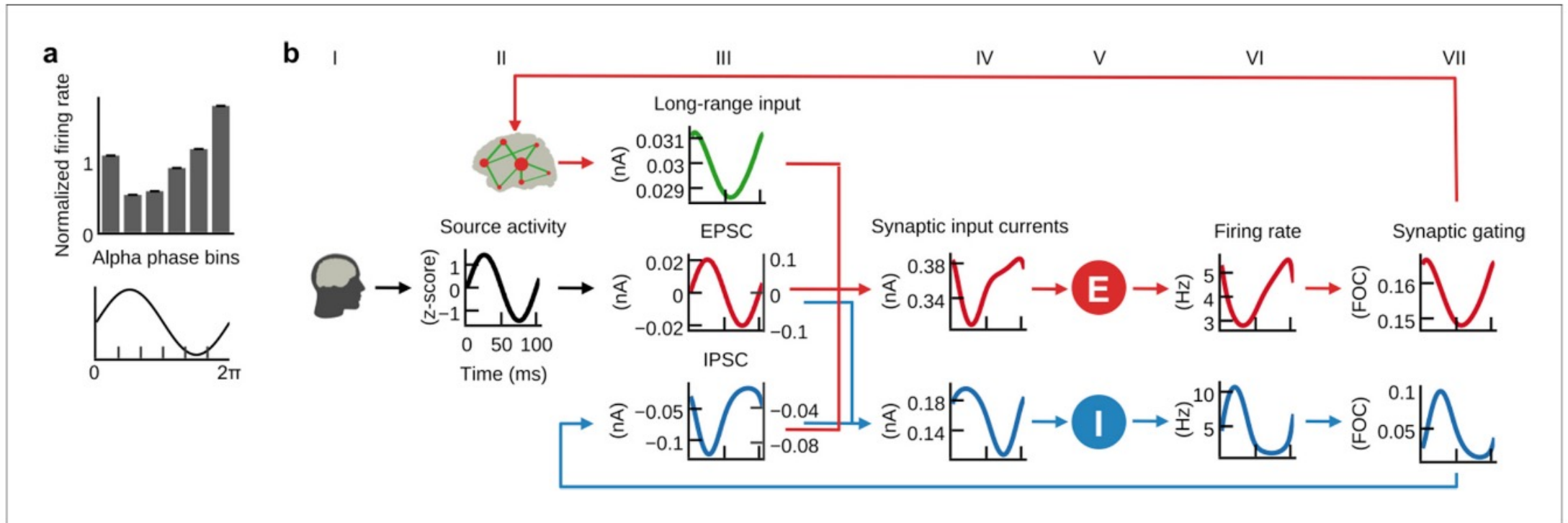
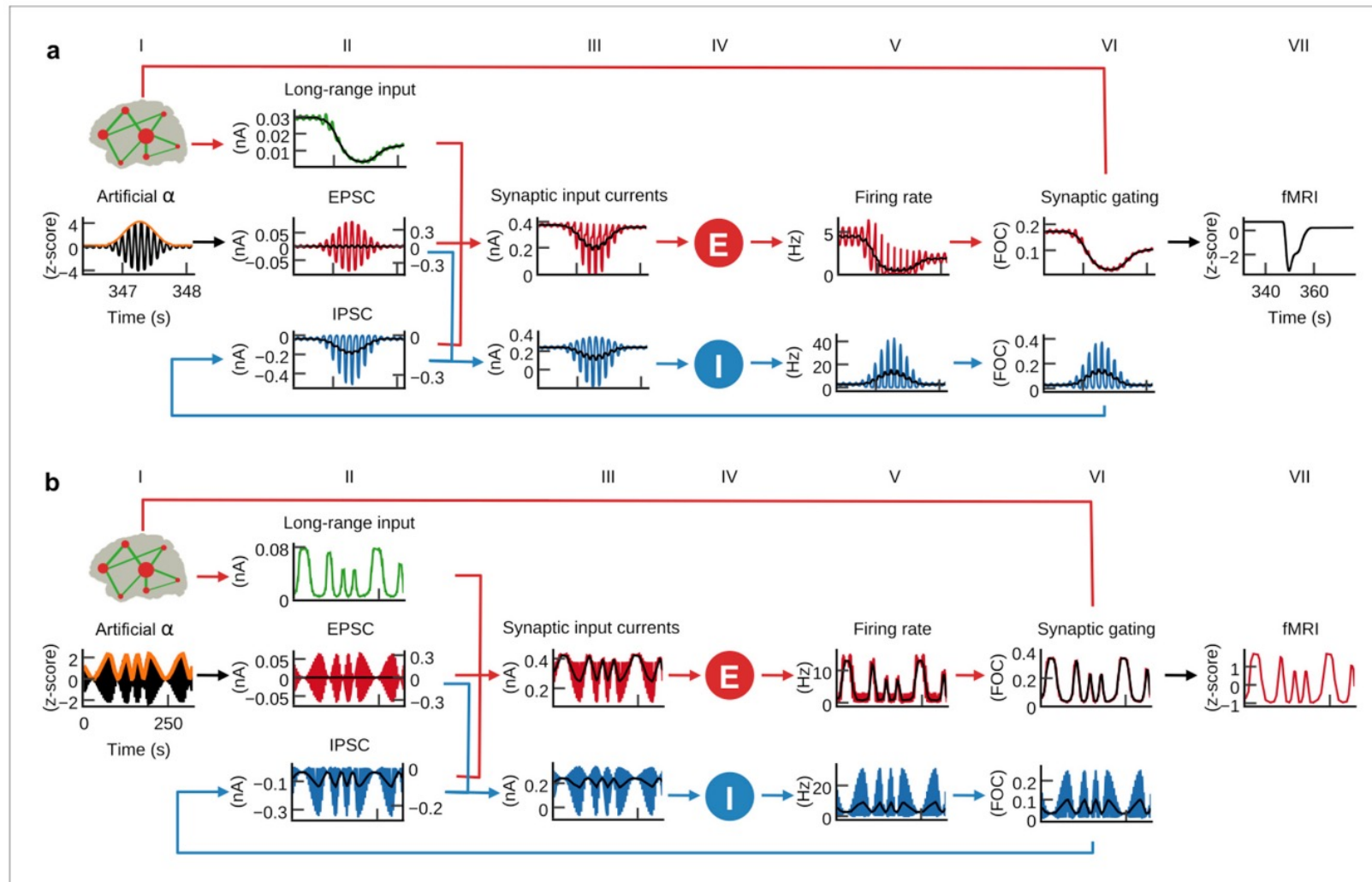
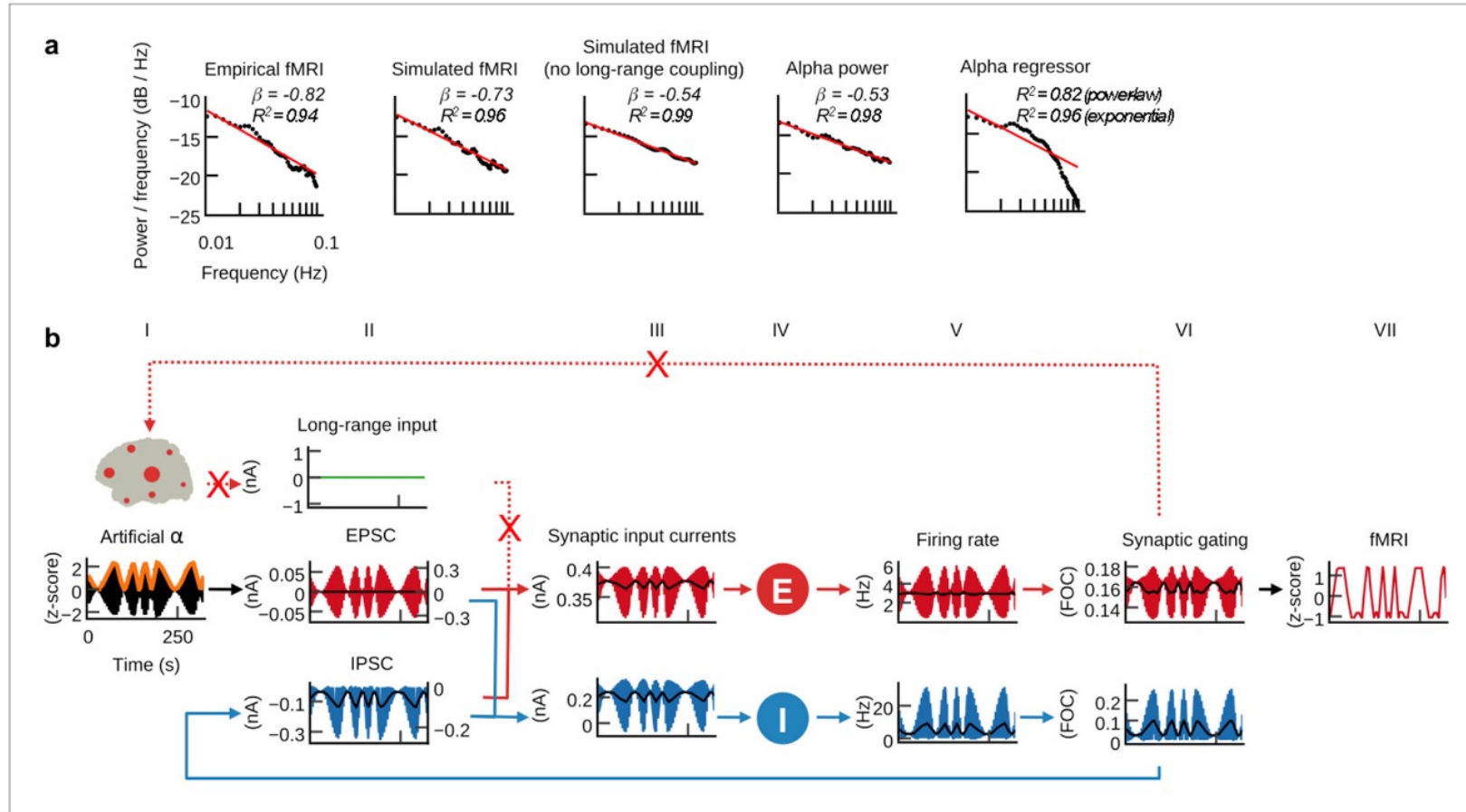


Fig 6. Alpha-power fluctuation generate fMRI





# Fig 7. Long-range coupling control power-law



# E/I balance generates the inverse relationship between alpha-phase and firing

- Alpha-cycle has inversed relationship with excitatory activities of neuronal population
- It exists a feedback loop between excitatory and inhibitory neuronal activities
- Long-range input play critical role on increasing amplitude during **\*\*slower\*\*** alpha-band power modulation.
- A power law distribution

# Equations

$$I_i^{(E)} = W_E I_0 + G \sum_j C_{ij} S_j^{(E)} - J_i S_i^{(I)} + w_{BG}^{(E)} I_{BG}$$

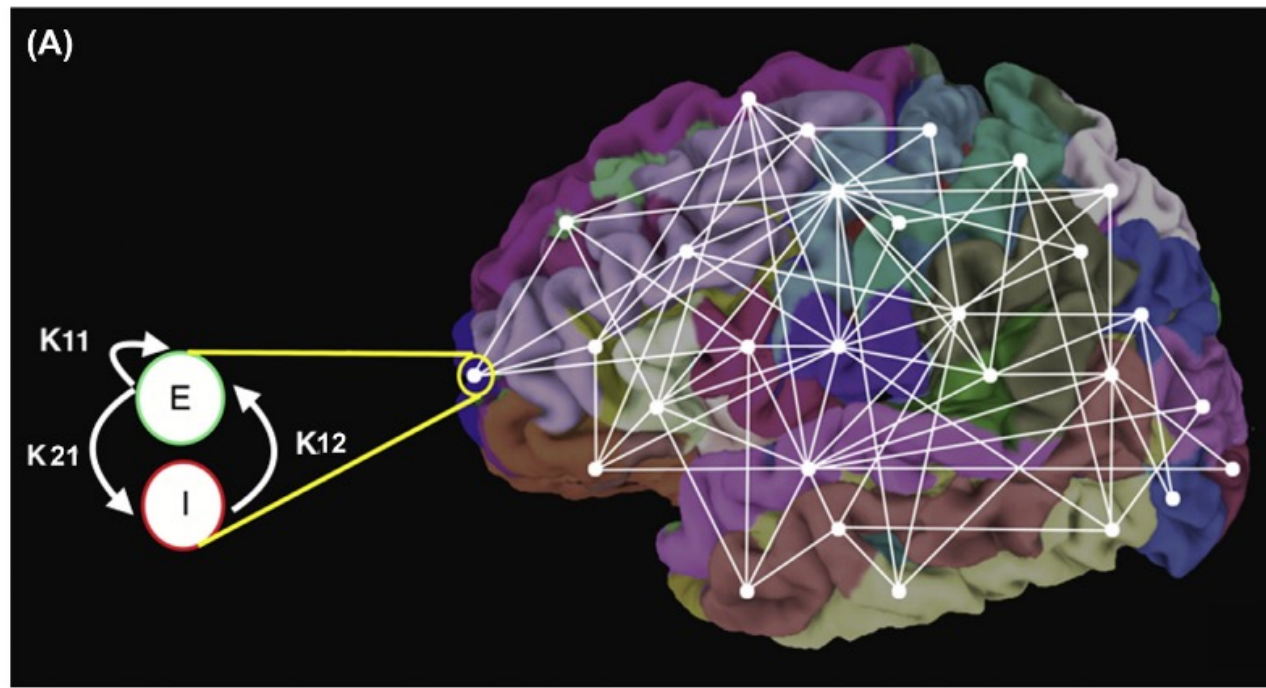
$$I_i^{(I)} = W_I I_0 - S_i^{(I)} + w_{BG}^{(I)} I_{BG}$$

$$r_i^{(E)} = \frac{a_E I_i^{(E)} - b_E}{1 - \exp\left(-d_E \left(a_E I_i^{(E)} - b_E\right)\right)}$$

$$r_i^{(I)} = \frac{a_I I_i^{(I)} - b_I}{1 - \exp\left(-d_I \left(a_I I_i^{(I)} - b_I\right)\right)}$$

$$\frac{dS_i^{(E)}(t)}{dt} = -\frac{S_i^{(E)}}{\tau_E} + \left(1 - S_i^{(E)}\right) \gamma_E r_i^{(E)}$$

$$\frac{dS_i^{(I)}(t)}{dt} = -\frac{S_i^{(I)}}{\tau_I} + \gamma_I r_i^{(I)}$$



(B)

$$\frac{dx_i(t)}{dt} = N(x_i(t)) + G \sum_j SC_{ij} x_j(t - d_{ij}^{glob}) + L \sum_j LC_{ij} x_j(t - d_{ij}^{loc}) + I_i(t) + v_i(t)$$

Differential operator that maps the system of equations into its derivatives

State operator for each neural mass  $i$  (i.e., neural mass model).

Vector of state variables for each region  $i$ , e.g., synaptic activity, firing rates, mean field

Global coupling scaling factor

Structural connectivity matrix (global coupling)

Time delays

Local connectivity

Injected input

Noise